AGU PUBLICATIONS

JGR

Journal of Geophysical Research: Space Physics

RESEARCH ARTICLE
10.1002/2016JA023477

Key Points:
- Observations of Pc5 waves in the polar cap by ground magnetometers and in the near-cusp ionosphere by SuperDARN radars
- Signatures at the footprint of open field lines of FLRs occurring at lower latitudes
- Direct transmission of waves from the solar wind into the Earth's magnetosphere

Correspondence to:
M. De Lauretis,
marcello.delauretis@aquila.infn.it

Citation:
De Lauretis, M., M. Regi, P. Francia, M. F. Marcucci, E. Amata, and G. Pallocchia (2016), Solar wind-driven Pc5 waves observed at a polar cap station and in the near cusp ionosphere, *J. Geophys. Res. Space Physics*, *121*, doi:10.1002/2016JA023477.

Received 19 SEP 2016
Accepted 10 NOV 2016
Accepted article online 15 NOV 2016

Solar wind-driven Pc5 waves observed at a polar cap station and in the near cusp ionosphere

M. De Lauretis[1], M. Regi[1], P. Francia[1], M. F. Marcucci[2], E. Amata[2], and G. Pallocchia[2]

[1]Department of Physical and Chemical Sciences, University of L'Aquila, L'Aquila, Italy, [2]IAPS-INAF, Rome, Italy

Abstract We present the results of a comparative study conducted in Antarctica by using the ULF geomagnetic field measurements at Terra Nova Bay (Altitude Adjusted Corrected Geomagnetic Coordinates latitude 80°S) and simultaneous data from the Super Dual Auroral Radar Network radar at South Pole Station. Pc5 waves observed at Terra Nova Bay around local magnetic noon, when the station is close to the dayside cusp, can be interpreted as spatial integrated signals, produced by ionospheric currents associated to field line resonances at somewhat lower latitudes. The radar, providing the Doppler velocities of ionospheric plasma over a range of geomagnetic latitudes, allows to detect the occurrence of such field line resonances. In the reported case, our analysis shows evidence of resonant signals in the ionosphere at 75°S and 76°S that find correspondence in frequency and time with the geomagnetic signals observed at Terra Nova Bay around local noon. During the period of interest, oscillations of the solar wind dynamic pressure at the same frequency are detected by Geotail, just upstream of the morning flank of the bow shock. All the observations are consistent with the interpretation of the signals at Terra Nova Bay in terms of signatures of field line resonances occurring at lower latitudes, driven by solar wind oscillations transmitted into the magnetosphere. We discuss also the possibility of an additional contribution to the signals at Terra Nova Bay, due to the direct propagation of the solar wind waves along the local open field line.

1. Introduction

In our previous studies, based on ULF geomagnetic measurements at Terra Nova Bay (TNB) in Antarctica (Altitude Adjusted Corrected Geomagnetic Coordinates (AACGM) latitude ~80°S, magnetic local time (MLT) ~ UT-08), we found a significant wave activity in the Pc5 frequency range (1–7 mHz), more pronounced around local magnetic noon (~20:00 UT), when the station is located near the dayside cusp and outermost closed field lines [*Villante et al*., 2000; *Francia et al*., 2005, 2009].

The study of the polarization characteristics of Pc5 waves is useful to obtain information on their generation and propagation in the magnetosphere. Waves originated by a solar wind (SW)-driven process, for example the Kelvin-Helmholtz instability, the impact of SW pressure pulses, or the direct transmission of SW fluctuations [*Menk*, 2011; *Regi et al*., 2015], propagate in the antisunward direction, i.e., westward in the local morning and eastward in the afternoon. The resulting polarization sense of ground measurements should be (looking downward in the southern hemisphere) clockwise (CW) in the morning and counterclockwise (CCW) in the afternoon. In addition, it has been demonstrated that when the compressional waves couple with the Alfvén modes at the matching frequencies, the polarization sense reverses at Λ_R, the latitude of the resonance, and at Λ_m, the latitude of the minimum amplitude between the resonant field line and the magnetopause [*Southwood*, 1974; *Chen and Hasegawa*, 1974]. At high latitudes, since in the outer magnetosphere the field lines are stretched on the flanks [*Waters et al*., 1995; *Mathie et al*., 1999], both Λ_R and Λ_m are higher at noon with respect to dawn and dusk. Such diurnal variation is consistent with the original results by *Samson et al*. [1971] and *Samson* [1972], who analyzed the polarization of Pc5 pulsations at northern geomagnetic latitudes between 59° and 77°.

Statistical analyses of the polarization of Pc5 pulsations at TNB [*Lepidi et al*., 1999; *Villante et al*., 2009; *Francia et al*., 2009] reveal a station generally situated poleward with respect to Λ_m except in the noon sector, when it is close to the resonant latitude Λ_R. In particular, four polarization reversals appear through the day: in the premidnight and postmidnight sectors the observed polarization sense is consistent with an antisunward propagation, while in the prenoon and postnoon hours it is respectively CCW and CW; this feature suggests that in the dayside, TNB moves into the region between Λ_m and Λ_R, where the effects of field line resonances (FLRs) occurring at somewhat lower latitude can still be observed ("resonance region"). Indeed, in the

ionosphere, the ULF electric field generates horizontal currents with a finite scale size, which in turn produce magnetic signals; due to the integrated view over the sky, a ground magnetometer measures the superposition of such magnetic signals, with each contribution weighted according to the Biot-Savart law [*Hughes and Southwood*, 1976; *Poulter and Allan*, 1985; *Ponomarenko et al*., 2001]. In this sense, the FLR signals are "smeared" at the ground by the ionosphere and can be observed at TNB.

ULF pulsations can also be studied by using ionospheric radars. They provide line-of-sight Doppler velocities of the ionospheric plasma along adjacent beams, exploring different latitudes and longitudes. FLRs cause oscillations in the ionospheric plasma flows by the $\boldsymbol{e} \times \boldsymbol{B}$ drift, where $\boldsymbol{e}$ is the ULF electric field and $\boldsymbol{B}$ is the local field, and thus, they can be detected in the measured Doppler velocities along the east-west direction [*Samson et al*., 1992; *Fenrich et al*., 1995; *Stephenson and Walker*, 2002; *Nedie et al*., 2012]. Both in the northern and southern polar caps, several radars of the Super Dual Auroral Radar Network (SuperDARN) network are now operating, allowing a useful comparison with magnetometer data.

In this study we present an analysis of ULF fluctuations measured in the geomagnetic field at TNB around local magnetic noon and simultaneous ionospheric flow oscillations measured by the SuperDARN radar at South Pole Station, which explores, approximately along the azimuthal direction, the ionosphere over a range of latitudes slightly lower than TNB. The ULF event was observed on 27 March 2013, during the time interval 18:00–22:00 UT and is characterized by ~2 mHz oscillations before and after 20:00 UT. We show that the TNB fluctuations, whose polarization sense is consistent with resonance effects, find a clear correspondence with the ionospheric plasma velocity oscillations along the east-west direction, which are associated to FLRs, at latitudes of ~76°S and 75°S. Such result is consistent with our interpretation of low-frequency fluctuations observed at TNB around the local magnetic noon in terms of signatures of the FLR occurring at lower latitude. During the period of interest, the observed occurrence of SW dynamic pressure fluctuations at the same frequency leads to the conclusion that they are the source of the TNB fluctuations, driving the FLR after transmission into the dayside magnetosphere. We discuss also the possibility of an additional contribution to the signals at Terra Nova Bay, due to the direct propagation of the SW waves along the local open field lines.

2. Observations

2.1. Magnetometer Data

We analyzed the ULF geomagnetic field measurements at the Italian base "Mario Zucchelli" at TNB. The equipment consists of a high-sensitivity induction coil measuring the geomagnetic field fluctuations in the northward (*H*), eastward (*D*), and vertically downward (*Z*) components, at sampling rate of 1 s. We applied the wavelet spectral analysis to the whole data set to show the frequency/time evolution of the signals; we used the Morlet wavelet with dimensionless frequency $\omega_0 = 6$, so that the Fourier period almost coincides with the scale of the wavelet [*Torrence and Compo*, 1998].

In Figure 1 (top) we show the original time series and the 1–7 mHz filtered data during the time interval 18:00–22:00 UT on 27 March 2013. Low frequency, almost monochromatic oscillations in the *H* and *D* components, can be clearly observed just after 18:30 UT and between 21:00 and 21:30 UT. In correspondence, the wavelet spectra, shown in Figure 1 (middle), exhibit a power peak at ~2 mHz in the time interval 18:30–18:45 UT, more pronounced in the *D* component, and 21:00–21:30 UT. In the latter interval, both the *H* and *D* spectra show around 21:20 UT a broadband (up to 5 mHz) enhanced power.

Then, we computed running (with a step size of 15 min), 1 hr Fourier spectra and cross spectra between the horizontal components, frequency smoothed by a triangular filter over five adjacent frequency bands. We used the cross spectra to estimate the polarization parameters by means of the *Fowler et al*. [1967] spectral method, evaluating, for each frequency, the polarization ratio *R* (the ratio of the polarized and total intensity of the horizontal signal) and the ellipticity ε (the ratio of the minor and the major axis of the polarization ellipse in the horizontal plane), with positive/negative ε corresponding to CW/CCW sense. We found that the polarization ratio *R* is higher than 0.9 only during the time intervals 18:00–19:00 and 20:45–21:45 UT, i.e., when the clearer waveforms are observed in the filtered series. In Figure 1 (bottom) the power spectra and the ellipticity are plotted for such two intervals. The 18:00–19:00 UT spectra reveal, in both components, the presence of power peaks at ~2.0 mHz and, much lower, at ~3.3 mHz. The 20:45–21:45 UT spectra show a clear power peak at ~2.0 mHz in both components and an additional peak at ~3.9 mHz in the *D* component.

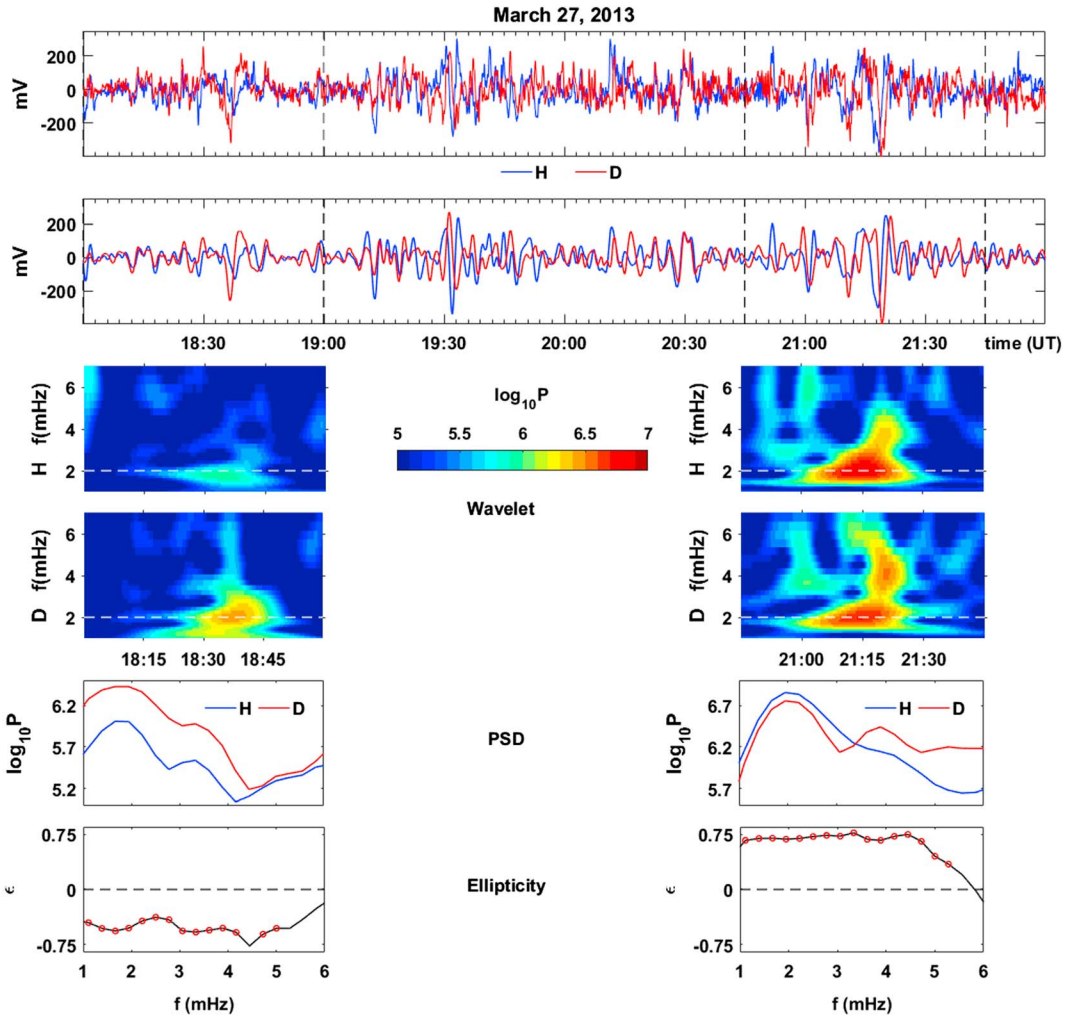

Figure 1. (top) The original and 1–7 mHz filtered magnetometer data at TNB during the time interval 18:00–22:00 UT on 27 March 2013. (middle) The dynamic wavelet power spectra of the *H* and *D* components for time intervals 18:00–19:00 UT and 20:45–21:45 UT. (bottom) The power spectra and the corresponding ellipticity values (the red points correspond to the polarization ratio higher than 0.9) for time intervals 18:00–19:00 UT and 20:45–21:45 UT.

In correspondence to the observed power peaks, the ellipticity is negative in the first time interval before local magnetic noon (20:00 UT = 12:00 MLT), while it is positive during 20:45–21:45 UT. Indeed, also, a visual inspection of the low-pass-filtered data shows that *D* preceded *H* around 18:30 UT, while it was somewhat delayed after 21:00 UT. The observed ellipticity indicates CCW polarized fluctuations before noon and CW polarized fluctuations in the afternoon, consistently with signatures of FLRs occurring on closed field lines at slightly lower latitudes.

2.2. Radar Data

For the examined event, data from the SuperDARN radar at South Pole Station (SPS) were available. The radar explores, across the magnetic meridians, a large portion (~03:00 MLT hours) of the ionosphere overlying the regions between 80°S and 70°S AACGM latitudes. It operates through 16 beams separated by 3.24° in azimuth with a total scan time of 1 min for the whole field of view. Each beam is divided into 75 gates. We used the line-of-sight Doppler velocities, i.e., the ionospheric plasma velocity component along the beams. The data have been interpolated to fill in small data gaps.

In Figure 2 (left), we show the spectral power at ~2.0 mHz during 18:00–19:00 UT, computed by the Fourier analysis, as seen in the field of view of the radar. Although the wave power is spread over a range of latitudes

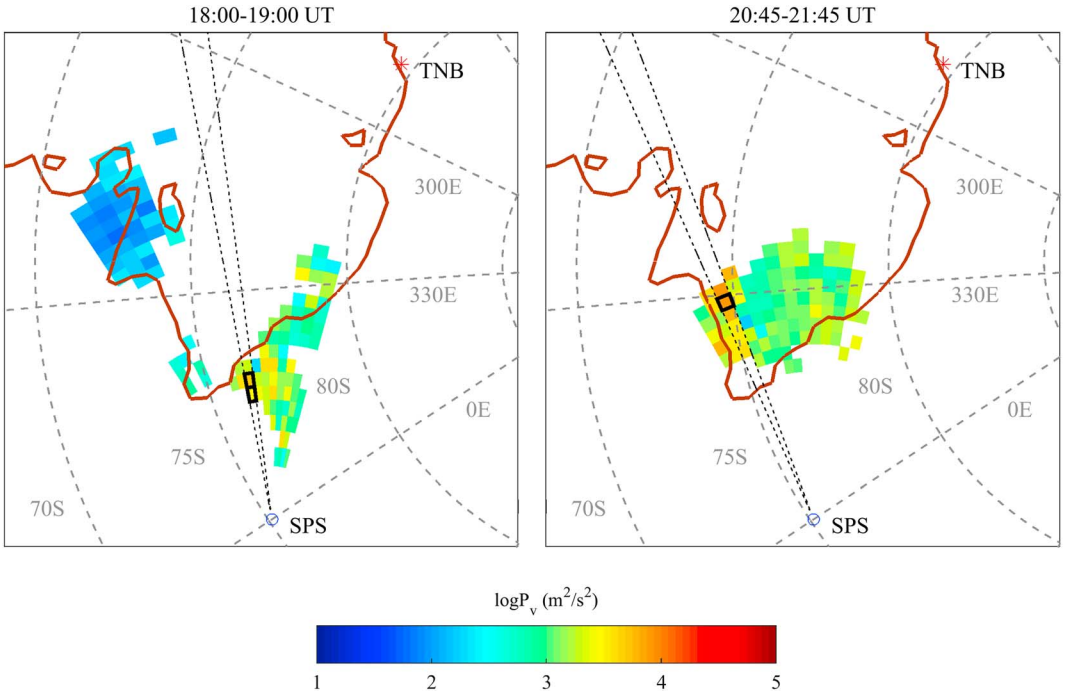

Figure 2. The spectral power of 2.0 mHz Doppler velocity as seen in the field of view of the SPS radar during the time intervals (left) 18:00–19:00 UT and (right) 20:45–21:45 UT on 27 March 2013, in geomagnetic coordinates. Beam 7, gates 9 and 10 and beam 11, gate 17 are evidenced respectively in the left and right figures.

(76°S–78°S), it appears higher at the geomagnetic latitude of 76°S. In particular, a higher power is observed along the beam 7 at the gates 9 and 10, where the beam is most closely aligned to the east-west direction, thus measuring plasma flow velocities associated with FLRs. As an example, in Figure 3a, we show the Doppler velocities (original and filtered data series) for beam 7, gates 9 and 10 (for this interval, in order to further reduce the number of gaps, we used data of gate 9 or gate 10 or their average, depending on availability). It the time interval 18:00–19:00 UT, it can be seen that the velocity fluctuations observed after 18:30 UT exhibit a close correspondence with the low-frequency variations of the TNB geomagnetic field in the same time interval, especially in the *D* component. The corresponding wavelet spectrum (Figure 3a, bottom) shows a clear power peak around 2 mHz between 18:30 and 18:45 UT. It is worth to note that such spectral structure is very similar to the one observed at TNB in the *D* component of the geomagnetic field fluctuations.

For the time interval 20:45–21:45 UT the spectral power at ~2.0 mHz is shown in the field of view of the radar in Figure 2 (right). In this case, the highest power is observed at geomagnetic latitudes around 75°S, particularly in correspondence to beam 10, gate 19 and along beam 11, gates 16—18, which are roughly aligned with the relative magnetic shell. In Figure 3b we show the Doppler velocities (original and filtered data series) for beam 11, gate 17. In the time interval 20:45–21:45 UT the line-of-sight velocity shows large fluctuations, as simultaneously observed in the geomagnetic field. The wavelet spectrum (Figure 3b, bottom) is characterized by two power enhancements: the first emerges at 3–4 mHz between 21:00 and 21:10 UT, while the second, at ~2.0 mHz, extends from 21:10 to 21:30 UT.

In order to clearly associate the observed spectral features to FLRs, we examined the latitudinal dependence of the 2.0 mHz power and the corresponding phase variation in the SuperDARN data. We analyzed only the 20:45–21:45 UT time interval for which there is a latitudinal good data coverage (Figure 4). A FLR is characterized by a narrow power maximum and a 180° phase shift across this maximum [*Samson et al*., 1992; *Fenrich et al*., 1995; *Nedie et al*., 2012]. Actually, we found that the power shows a narrow peak at the latitude of ~75°S, in correspondence to an ~200° phase decrease across the peak. Moreover, we used signals at longitudinally spaced gates along the 75°S shell, where enhanced power was observed, to estimate the azimuthal wave number (Figure 5). The phase-longitude relation is linear ($r = 0.95$), and the slope provides an azimuthal

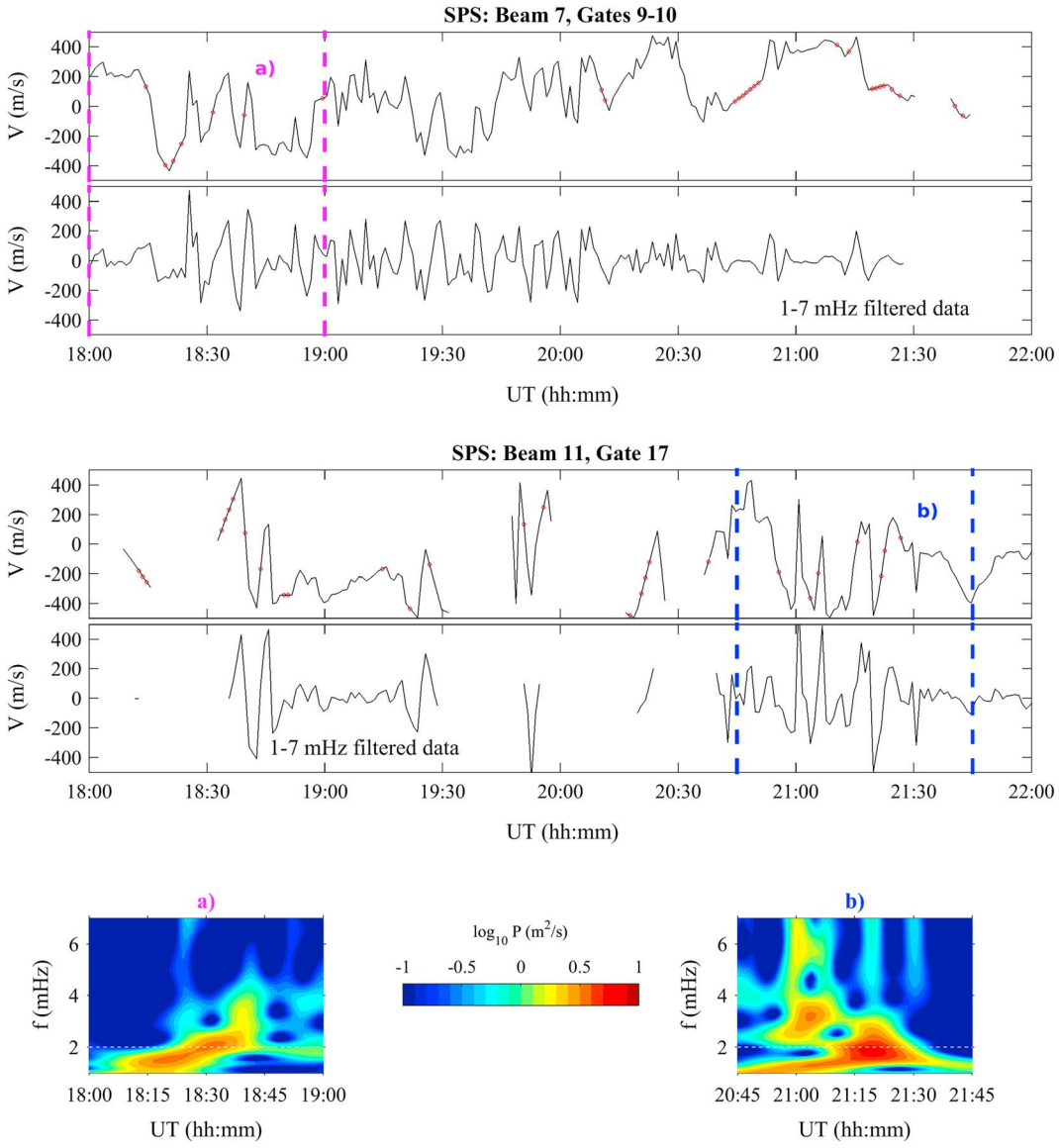

Figure 3. (top and middle) The original and 1–7 mHz filtered Doppler velocities for beam 7, gates 9 and 10 and for beam 11, gate 17, on 27 March 2013. Interpolated data gaps are indicated by red points; a good data coverage is evident during the two analyzed time intervals. (bottom) The wavelet spectra during the time interval (left) 18:00–19:00 UT and during the time interval (right) 20:45–21:45 UT.

$m \sim 14 \pm 2$, indicating that we are observing a low-m resonance [*Fenrich et al.*, 1995]; it corresponds to a westward phase velocity of 1.5 km/s at the ionosphere.

Accordingly with the analysis results, for the two examined time intervals we tentatively identified FLRs at ~76°S and, more clearly, at 75°S where, under quiet geomagnetic conditions, waves with a frequency of ~2 mHz typically couple to FLRs in the noon sector [*Waters et al.*, 1995; *Mathie et al.*, 1999]. The slight decrease with time of the resonance latitude observed in Figure 2 is consistent with the diurnal variation of the length of high-latitude field lines; therefore, for a given frequency a FLR occurs at higher latitude close to the local noon with respect to the morning and the afternoon [*Samson*, 1972]; in our case, the examined ionospheric plasma oscillations occur in the postnoon sector during 18:00–19:00 UT and in the afternoon during 20:45–21:45 UT.

In order to put our observations in a general context, we used all available southern hemisphere SuperDARN observations to generate the maps of the global ionospheric convection for the two ULF observations. Such

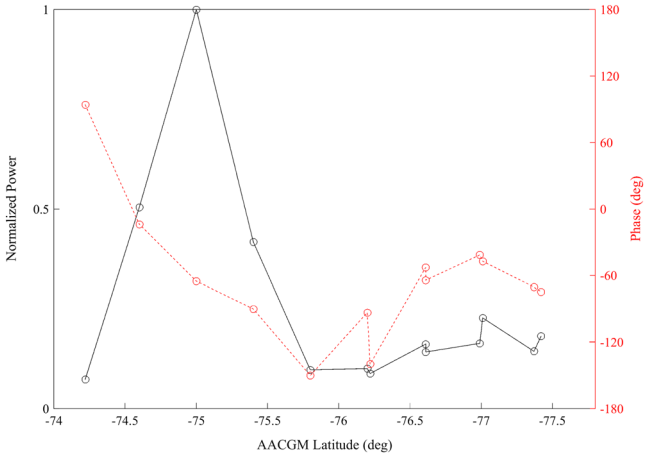

Figure 4. The latitudinal dependence of the 2 mHz power (black line) and the corresponding phase variation (red dotted line) for the 20:45–21:45 UT time interval.

maps are produced by using the potential mapping method by *Ruohoniemi and Baker* [1998]. This method expresses the electrostatic potential as an expansion in spherical harmonic functions with coefficients set so as to minimize the differences with the observations. The method makes use of data points from an empirical statistical model of the convection pattern, parameterized by the upstream interplanetary magnetic field (IMF), in regions where there are no observations. We used the magnetic field measured by the MGF experiment on board the Geotail spacecraft (at GSE [24,–9, 9] R_E) as input to the statistical model. The convection maps are available at 2 min intervals. The visual inspection of all the maps relative to the period of interest shows that the convection maps of 18:30 and 21:24 UT, displayed in Figure 6, represent well the convection configuration for the 18:00–19:00 and 21:14–22:00 UT intervals, respectively. Looking at the maps, it can be noted that the convection shows a two cell pattern with antisunward flows across the polar cap. The two cell pattern is rotated toward earlier MLT in both maps, more at 21:24 UT. During the corresponding periods the IMF observed by Geotail is characterized by a dominant B_y negative component (B_y-). More specifically the IMF is B_y- dominated with B_z slightly positive during the 18:00–19:00 UT interval and B_z slightly negative during the 21:14–22:00 UT interval.

From the above observations, we can conclude that the dayside ionospheric convection during the ULF events can be interpreted as due to reconnection taking place at the dayside magnetopause. In particular, the convection patterns are consistent with reconnection occurring at the dayside dusk high-latitude region in the southern hemisphere for the B_y- periods 18:00–19:00 and 21:14–22:00 UT [*Crooker*, 1979; *Reiff and Burch*, 1985; *Ruohoniemi and Greenwald*, 1996, 2005; *Pettigrew et al*., 2010].

In the maps we also show the precipitating particle data from the low-altitude NOAA Polar-Orbiting Operational Environmental Satellites (POES) and a proxy of the open-closed magnetic field line boundary (OCB). In particular, the 50–20,000 eV proton plus electron omni-directional energy flux, denominated Total Energy Detector Average (TEDA), from the Total Energy Detector instrument is superimposed to the satellite trajectories in the time intervals of interest. The poleward boundary of the high TEDA values gives a proxy of the OCB at a specific magnetic latitude and MLT for each of the satellites. The OCB latitudes at each MLT hour from 0 to 23 is then estimated by fitting the locations where the logarithm of the TEDA flux falls below −1.2 to a cosine function, in a similar way to that used by *Clausen et al*. [2012] to estimate the size of the R1 oval starting from the Active Magnetosphere and Planetary Electrodynamics Response Experiment

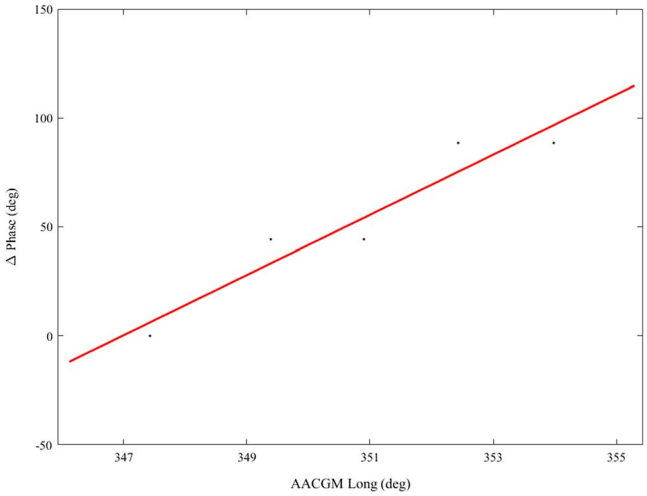

Figure 5. The longitudinal dependence of the phase for the 2 mHz resonance during the 20:45–21:45 UT time interval (beam 10, gate 19 and beam 11, gates 15–18).

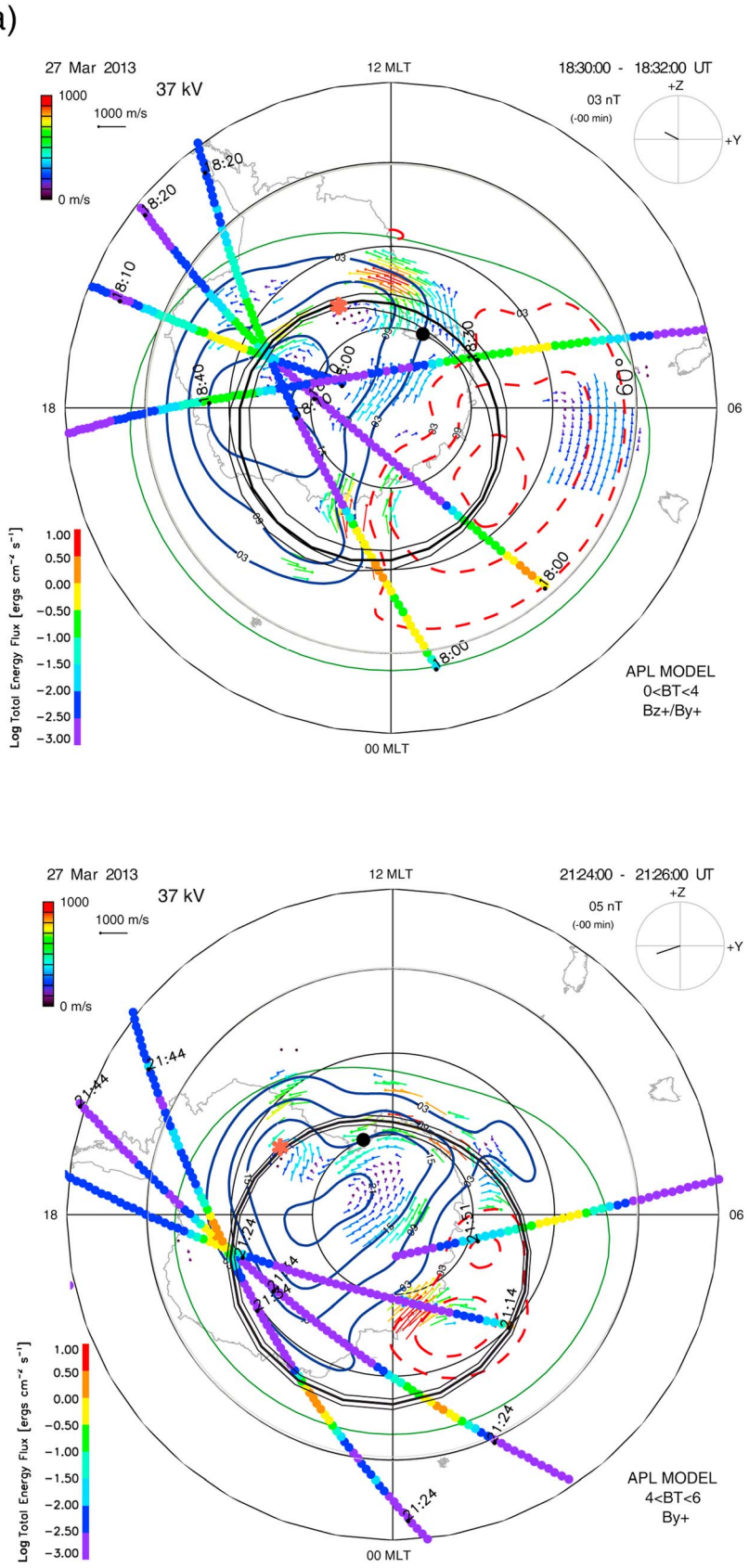

Figure 6. Global ionospheric convection maps for 2 min intervals starting at (a) 18:30 UT and (b) 21:24 UT.

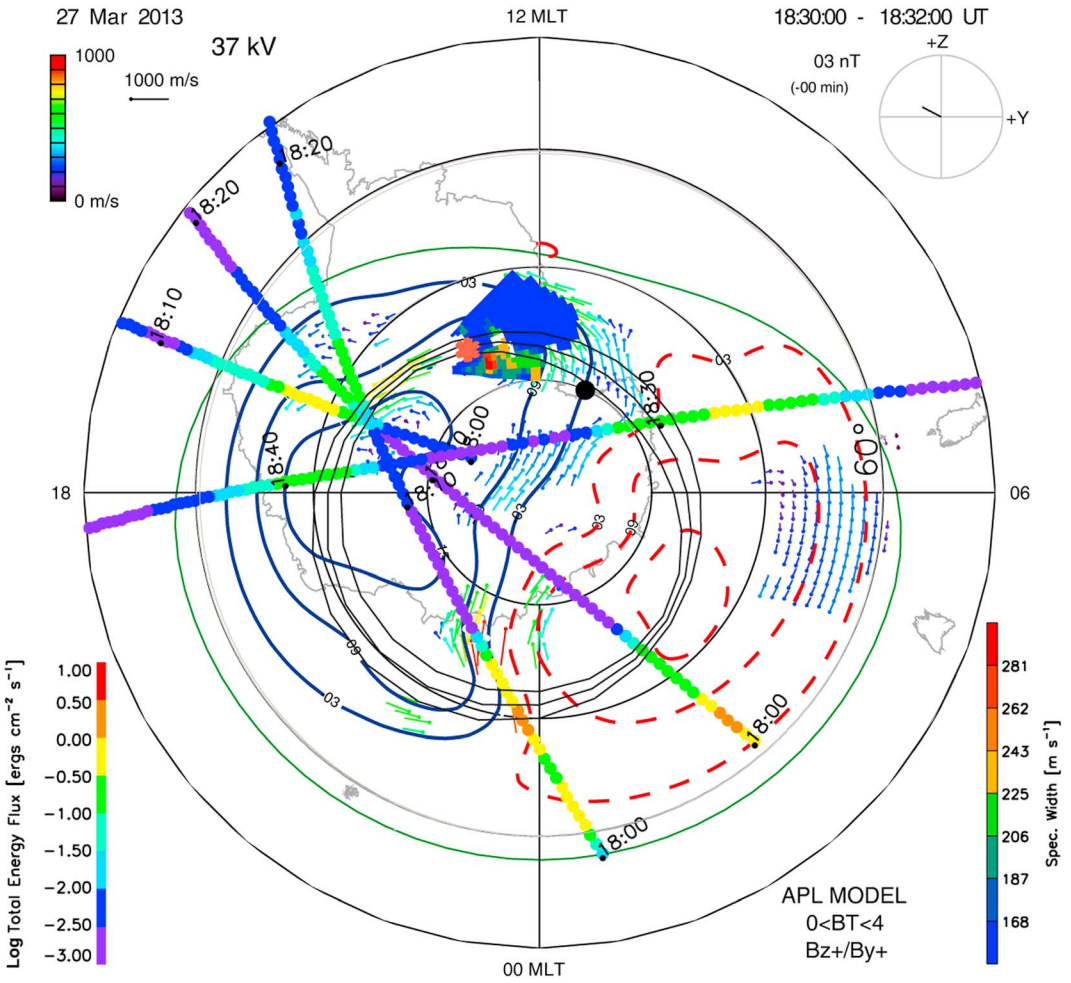

Figure 7. The South Pole Doppler spectral width measurements overplotted on the convection map of 18:30 UT.

field-aligned current densities. The cosine function describes an oval displaced from the magnetic pole. The mean latitude, the amplitude, and the phase of the displacement are free parameters, which are determined by minimizing the variance between the cosine function and the POES TEDA cutoff locations. The results of the fit are represented by the black solid oval. The two light ovals indicate the uncertainty on the position of the OCB, which is derived from the uncertainties on the latitudes of the POES satellite OCB crossings. These are estimated as the difference in latitude relative to the poleward transition from high to low TEDA values for each crossing. In particular, they correspond to the difference between the latitudes of the −0.75 and −1.75 cutoffs of the TEDA logarithm values. It can be seen that in the second interval, characterized by a slightly negative B_z, the predicted oval extends to lower latitudes than during the first interval.

In both time intervals, TNB (indicated in the maps by a black circle) is located within the polar cap; on the other hand, the 2 mHz maximum power of the ionospheric velocity fluctuations (marked by a red star) is observed close to the predicted OCB and closed field lines.

Moreover, in Figure 7 we show the South Pole Doppler spectral width measurements over plotted on the convection map of 18:30 UT. The boundary between low and high Doppler spectral width has been found to be another proxy of the OCB [*Milan et al.*, 2003; *Chisham et al.*, 2007, and references therein]. It can be seen that moderate to high spectral width backscatter (≥150 m/s) and low spectral width backscatter (≤150 m/s) are approximately separated by the OCB fit. This is an indication that in the postnoon MLT sector, where no POES satellites passages are present, the actual OCB is located near the position inferred using the fitting procedure.

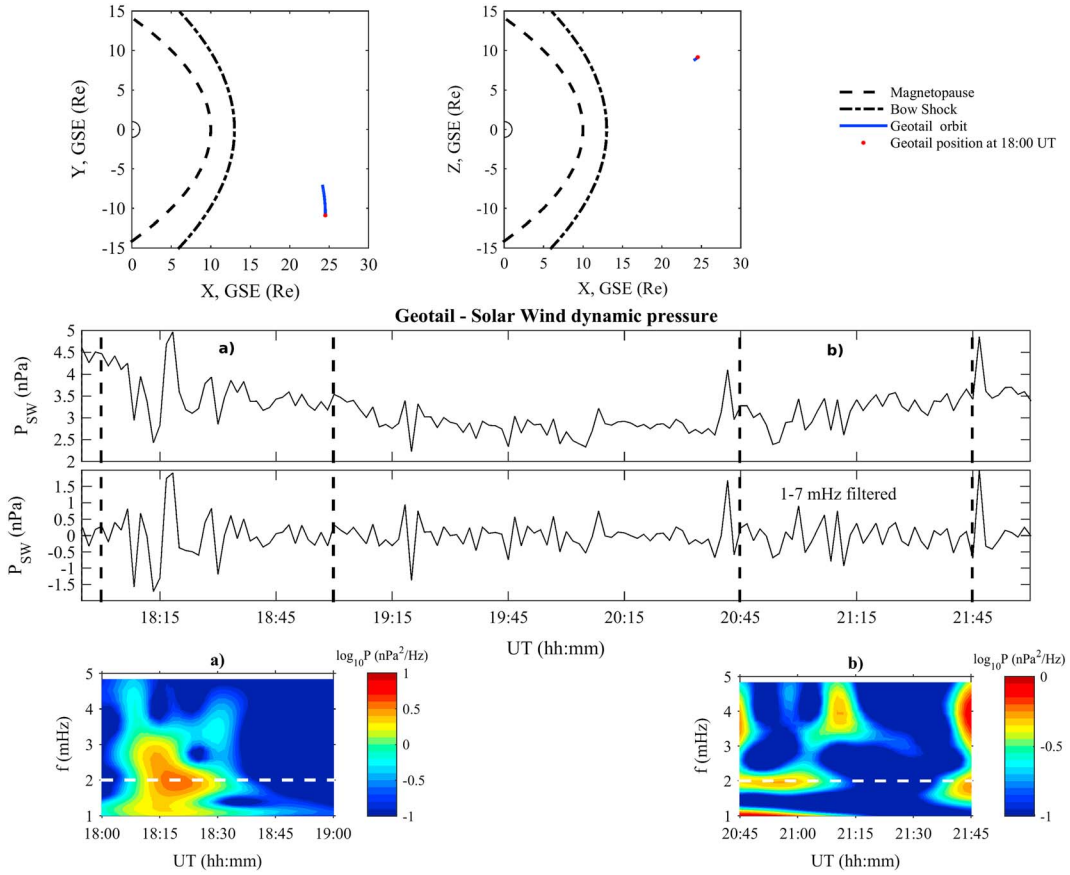

Figure 8. From the top: the position of Geotail during the time interval 18:00–22:00 UT; the SW dynamic pressure original data and the 1–7 mHz filtered series; the wavelet spectra during the time interval (left) 18:00–19:00 UT and during the time interval (right) 20:45–21:45 UT.

2.3. Solar Wind Data

In order to understand the origin of the pulsations, we analyzed the SW data from Geotail, which was located upstream of the Earth's bow shock, in the morning side (Figure 8, top).

In Figure 8 (middle) we show the original and filtered data series, and in Figure 8 (bottom) the wavelet spectrum of the SW dynamic pressure in the two intervals of interest. Between 18:15 and 18:30 UT it can be seen the presence of a 2 mHz power enhancement which, taking into account an estimated transit time of ~15 min from Geotail to ground [*Lockwood et al*., 1989, and references therein], can be associated to the power peak observed in the geomagnetic field at TNB and in the ionospheric plasma flow measured by the SPS radar. During the 20:45–21:45 UT interval, a power peak appears up to 21:10 UT, quite corresponding to the spectral features observed in the SPS velocities and in the geomagnetic field. Thus, the SW pressure fluctuations seem to be the driver of the FLR at 2.0 mHz observed at ~76°S and 75°S. Such result represents a further evidence of Pc5 FLRs associated with SW fluctuations, as reported in previous papers [*Stephenson and Walker*, 2002; *Eriksson et al*., 2006; *Fenrich and Waters*, 2008] and carefully analyzed by *Stephenson and Walker* [2010].

3. Summary and Conclusions

In this paper we examined an ULF wave event observed at TNB, i.e., at the footprint of an open field line. The availability of measurements from a nearby SuperDARN radar allowed to investigate the simultaneous occurrence of fluctuations in the ionosphere at latitudes few degrees lower than TNB. We found the following:

1. The TNB fluctuations have a frequency of ~2 mHz and show a CCW polarization in the local morning and a CW polarization in the afternoon, consistently with the polarization sense expected for a FLR excited, at a latitude few degree lower than TNB, by 2 mHz waves propagating antisunward.

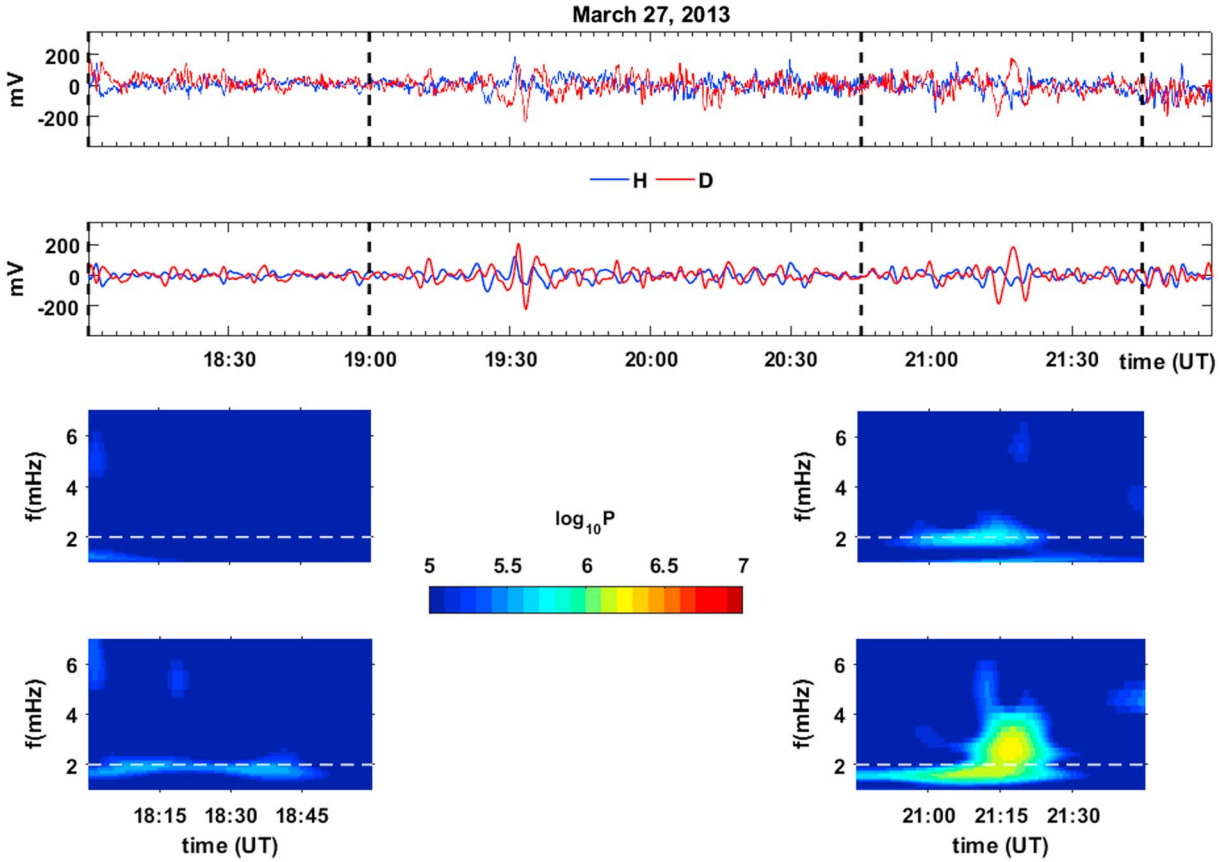

Figure 9. From the top: the original and 1–7 mHz filtered magnetometer data at DMC during the time interval 18:00–22:00 UT on 27 March 2013, the dynamic wavelet power spectra of the *H* and *D* components for time intervals 18:00–19:00 UT and 20:45–21:45 UT.

2. The analysis of data from the SPS radar clearly shows that the radar observed a 2 mHz power peak at ~76°S during the first time interval and at ~75°S during the second one, at longitudes where the beams are closely aligned with FLR-associated plasma flows; in particular, during the second time interval the plasma oscillations show typical signatures of a FLR characterized by a low *m*, corresponding to a westward phase velocity of ~1.5 km/s in the ionosphere; low-*m* FLR are generally thought as being generated by a SW source.
3. The OCB location is identified for both time intervals from the total proton and electron energy flux measurements provided by the POES satellite and is found consistent with closed field lines at ~76°S and ~75°S.
4. A direct penetration of waves from the SW into the magnetosphere can be suggested, since waves at approximately 2 mHz are detected in the SW dynamic pressure in the two time intervals.

On the basis of these results, we suggest that SW waves, transmitted across the dayside magnetopause and propagating through the magnetosphere, can excite FLRs on closed field lines with matching eigenfrequency (at the latitude of ~76°S and 75°S, respectively) and then signatures of such FLRs can be observed also at TNB, when the station is near the cusp and outermost closed field lines.

The correspondence between FLR associated signals in the ionosphere and fluctuations on open field lines just poleward of the cusp confirms therefore our interpretation of low-frequency (few mHz) fluctuations observed at TNB around local noon as signatures of FLRs occurring at somewhat lower latitude, due to the spatial integration and slow decay with distance of the signals produced by the ionospheric currents.

Finally, this effect could not be the only source of the fluctuations observed at TNB. Indeed, SW waves transmitted along open field lines could contribute directly to the TNB signals. Such transmission was observed by *Nedie et al*. [2012] in the northern polar cap, using data from multiple ground and space instrumentations.

On this regard, we found interesting to analyze, for a comparison, data from a magnetic station in the deep polar cap, far from closed field lines, during the examined event. We used data from Concordia station at Dome C (DMC, AACGM latitude ~89°S), located approximately at the geomagnetic pole. Figure 9 shows clear oscillations around 2 mHz, essentially during the 20:45–21:45 UT time interval, with amplitudes smaller than at TNB. We suggest that they are signatures of the SW driver waves, directly transmitted along the DMC open field line.

This result leads us to conclude that at TNB we can observe the effects of the FLR, excited on the outermost closed field lines by the SW waves propagating in the magnetosphere, and, in addition, of the direct transmission of the SW driver waves, their signatures being also observed up to the DMC field line, at least during the 20:45–21:45 UT interval.

Acknowledgments
This research was supported by the Italian PNRA (Programma Nazionale di Ricerche in Antartide). Magnetic field data at TNB can be requested to M. De Lauretis (marcello.delauretis@aquila.infn.it). The Geotail data are from CDAWeb. The authors acknowledge the use of SuperDARN data. SuperDARN is a collection of radars funded by the National Science Funding agencies of Australia, Canada, China, France, Japan, Italy, South Africa, United Kingdom, and United States of America. Operation of the South Pole SuperDARN radar was supported by grant the PLR09044270 from the United States National Science Foundation Division of Polar Programs.

References

Chen, L., and A. Hasegawa (1974), A theory of long period magnetic pulsations 1: Steady state excitation of field line resonance, *J. Geophys. Res.*, *79*, 1024–1037, doi:10.1029/JA079i007p01024.

Chisham, G., et al. (2007), A decade of the Super Dual Auroral Radar Network (SuperDARN): Scientific achievements, new techniques and future directions, *Surv. Geophys.*, *28*, 33–109, doi:10.1007/s10712-007-9017-8.

Clausen, L. B. N., J. B. H. Baker, J. M. Ruohoniemi, S. E. Milan, and B. J. Anderson (2012), Dynamics of the region 1 Birkeland current oval derived from the Active Magnetosphere and Planetary Electrodynamics Response Experiment (AMPERE), *J. Geophys. Res.*, *117*, A06233, doi:10.1029/2012JA017666.

Crooker, N. U. (1979), Dayside merging and cusp geometry, *J. Geophys. Res.*, *84*, 951–959, doi:10.1029/JA084iA03p00951.

Eriksson, P. T. I., A. D. M. Walker, and J. A. E. Stephenson (2006), A statistical correlation of Pc5 pulsations and solar wind pressure oscillations, *Adv. Space Res.*, *38*, 1763–1771, doi:10.1016/j.asr.2005.08.023.

Fenrich, F. R., and C. L. Waters (2008), Phase coherence analysis of a field line resonance and solar wind oscillation, *Geophys. Res. Lett.*, *35*, L20102, doi:10.1029/2008GL035430.

Fenrich, F. R., J. C. Samson, G. Sofko, and R. A. Greenwald (1995), ULF high- and low-m field line resonances observed with the Super Dual Auroral Radar Network, *J. Geophys. Res.*, *100*, 21,535–21,547, doi:10.1029/95JA02024.

Fowler, R. A., B. J. Kotick, and R. D. Elliott (1967), Polarization analysis of natural and artificially induced geomagnetic micropulsation, *J. Geophys. Res.*, *72*, 2871–2883, doi:10.1029/JZ072i011p02871.

Francia, P., L. J. Lanzerotti, U. Villante, S. Lepidi, and D. Di Memmo (2005), A statistical analysis of low frequency magnetic pulsations at South Pole, *J. Geophys. Res.*, *110*, A02205, doi:10.1029/2004JA010680.

Francia, P., M. De Lauretis, M. Vellante, U. Villante, and A. Piancatelli (2009), ULF geomagnetic pulsations at different latitudes in Antarctica, *Ann. Geophys.*, *27*, 3621–3629, doi:10.5194/angeo-27-3621-2009.

Hughes, W. J., and D. J. Southwood (1976), The screening of micropulsation signals by the atmosphere and ionosphere, *J. Geophys. Res.*, *81*, 3234–3240, doi:10.1029/JA081i019p03234.

Lepidi, S., P. Francia, U. Villante, L. J. Lanzerotti, and A. Meloni (1999), Polarization pattern of low frequency geomagnetic field fluctuations (0.8–3.6 mHz) at high and low latitude, *J. Geophys. Res.*, *104*, 305–310, doi:10.1029/1998JA900002.

Lockwood, M., P. E. Sandholt, and S. W. H. Cowley (1989), Interplanetary magnetic field control of dayside auroral activity and the transfer of momentum across the dayside magnetopause, *Planet. Space Sci.*, *37*, 1347–1365, doi:10.1016/0032-0633(89)90106-2.

Mathie, R. A., F. W. Menk, I. R. Mann, and D. Orr (1999), Discrete field line resonances and the Alfven continuum in the outer magnetosphere, *Geophys. Res. Lett.*, *26*, 659–662, doi:10.1029/1999GL900104.

Menk, F. W. (2011), Magnetospheric ULF waves: A review, in *The Dynamic Magnetosphere*, *IAGA Special Sopron Book Series 3*, edited by W. Liu and M. Fujimoto, pp. 223–256 .

Milan, S. E., M. Lester, S. W. H. Cowley, K. Oksavik, M. Brittnacher, R. A. Greenwald, G. Sofko, and J.-P. Villain (2003), Variations in the polar cap area during two substorm cycles, *Ann. Geophys.*, *21*, 1121–1140, doi:10.5194/angeo-21-1121-2003.

Nedie, A. Z., R. Rankin, and F. R. Fenrich (2012), SuperDARN observations of the driver wave associated with FLRs, *J. Geophys. Res.*, *117*, A06232, doi:10.1029/2011JA017387.

Pettigrew, E. D., S. G. Shepherd, and J. M. Ruohoniemi (2010), Climatological patterns of high-latitude convection in the Northern and Southern hemispheres: Dipole tilt dependencies and interhemispheric comparisons, *J. Geophys. Res.*, *115*, A07305, doi:10.1029/2009JA014956.

Poulter, E. M., and W. Allan (1985), Transient ULF pulsation decay rates observed by ground based magnetometers: The contribution of spatial integration, *Planet. Space Sci.*, *33*, 607–616, doi:10.1016/0032-0633(85)90046-7.

Ponomarenko, P. V., C. L. Waters, M. D. Sciffer, B. J. Fraser, and J. C. Samson (2001), Spatial structure of ULF waves: Comparison of magnetometer and Super Dual Auroral Radar Network data, *J. Geophys. Res.*, *106*, 10,509–10,517, doi:10.1029/2000JA000281.

Reiff, P. H., and J. L. Burch (1985), IMF By-dependent plasma flow and Birkeland currents in the dayside magnetosphere 2. A global model for northward and southward IMF, *J. Geophys. Res.*, *90*, 1595–1609, doi:10.1029/JA090iA02p01595.

Regi, M., M. De Lauretis, and P. Francia (2015), Pc5 geomagnetic fluctuations in response to solar wind excitation and their relationship with relativistic electron fluxes in the outer radiation belt, *Earth Planets Space*, *67*, 1–9, doi:10.1186/s40623-015-0180-8.

Ruohoniemi, J. M., and K. B. Baker (1998), Large-scale imaging of high latitude convection with Super Dual Auroral Radar Network HF radars observations, *J. Geophys. Res.*, *103*, 20,797–20,811, doi:10.1029/98JA01288.

Ruohoniemi, J. M., and R. A. Greenwald (1996), Statistical patterns of high-latitude convection obtained from Goose Bay HF radar observations, *J. Geophys. Res.*, *101*, 21,743–21,763, doi:10.1029/96JA01584.

Ruohoniemi, J. M., and R. A. Greenwald (2005), Dependencies of high-latitude plasma convection: Consideration of interplanetary magnetic field, seasonal, and universal time factors in statistical patterns, *J. Geophys. Res.*, *110*, A09204, doi:10.1029/2004JA010815.

Samson, J. C. (1972), Three-dimensional polarization characteristics of high latitude Pc5 geomagnetic micropulsations, *J. Geophys. Res.*, *77*, 6145–6160, doi:10.1029/JA077i031p06145.

Samson, J. C., J. A. Jacobs, and G. Rostoker (1971), Latitude-dependent characteristics of long period geomagnetic micropulsations, *J. Geophys. Res.*, *76*, 3675–3683, doi:10.1029/JA076i016p03675.

Samson, J. C., B. G. Harrold, J. M. Ruohoniemi, R. A. Greenwald, and A. D. M. Walker (1992), Field line resonances associated with MHD waveguides in the magnetosphere, *Geophys. Res. Lett.*, *19*, 441–444, doi:10.1029/92GL00116.

Southwood, D. J. (1974), Some features of field line resonance in the magnetosphere, *Planet. Space Sci.*, *22*, 482–491, doi:10.1016/0032-0633(74)90078-6.

Stephenson, J. A. E., and A. D. M. Walker (2002), HF radar observations of Pc5 ULF pulsations driven by the solar wind, *Geophys. Res. Lett.*, *29*(9), 1297, doi:10.1029/2001GL014291.

Stephenson, J. A. E., and A. D. M. Walker (2010), Coherence betweenradar observations of magnetospheric field line resonances and discrete oscillations in the solar wind, *Ann. Geophys.*, *28*, 47–59, doi:10.5194/angeo-28-47-2010.

Torrence, C., and G. P. Compo (1998), A practical guide to wavelet analysis, *Bull. Am. Meteorol. Soc.*, *79*, 61–78, doi:10.1175/1520-0477(1998)079<0061:APGTWA>2.0.CO;2.

Villante, U., S. Lepidi, P. Francia, M. Vellante, A. Meloni, and P. Palangio (2000), ULF fluctuations at Terra Nova Bay (Antarctica), *Ann. Geofis.*, *43*, 217–227.

Villante, U., P. Francia, M. Vellante, and M. De Lauretis (2009), Polarization pattern of low and mid-frequency magnetic pulsations in the polar cap: A comprehensive analysis at Terra Nova Bay (Antarctica), *Adv. Space Res.*, *38*, 1763–1771.

Waters, C. L., J. C. Samson, and E. F. Donovan (1995), The temporal variation of the frequency of high latitude field line resonances, *J. Geophys. Res.*, *100*, 7987–7996, doi:10.1029/94JA02712.